# FRESHWATER CRAYFISH CHITOSAN – A NOVEL SOURCE FOR NANOPARTICLE DEVELOPMENT: OPTIMIZATION, CHEMICAL MODIFICATIONS AND CHARACTERIZATION

MARIA MEMECICĂ,\* ANA-MARIA ALBU,\* NATALIA SIMIONESCU\*\*
DAMIEN CHAUDANSON\*\*\* and ALIN IONUŢ ALECU\*

\*National University for Science and Technology POLITEHNICA Bucharest, Faculty of Chemical Engineering and Biotechnologies, 1-7 Gh. Polizu Str., S1, 011061, Bucharest, Romania

\*\*"Petru Poni" Institute of Macromolecular Chemistry, Centre of Advanced Research in Bionanoconjugates and Biopolymers, 41A, Grigore Ghica Voda Alley, 700487 Iasi, Romania

\*\*\*\*Aix-Marseille Universite, CNRS, CINaM UMR 7325, 13288 Marseille, France

© Corresponding authors: M. Memecică, maria.memecica@yahoo.com

A.-M. Albu, anamaria.albu@upb.ro

In memoriam Acad. Bogdan C. Simionescu (1948-2024)

Advances in nanomedicine have demonstrated the reliability of using polymer-based nanoparticles as a material for effective drug delivery. In the context of sustainable development from renewable resources, the range of raw materials is diversified, focusing on natural resources. Chitosan is a promising resource for the development of nanoparticles with architectural-geometric versatility. Our study aims to demonstrate the viability of a new type of chitosan extracted from freshwater crayfish and its derivatives in obtaining nanoparticles. Polymer nanoparticles were characterized by dynamic scattering light spectroscopy (DLS), Fourier transform infrared spectroscopy (FTIR), electron scanning microscopy (SEM), electron transmission microscopy (TEM), and in terms of zeta potential (ZP). The mean size of nanoparticles was observed in the 59-74 nm homogeneous distribution range. The samples had relatively high positive values of zeta potential. *In vitro* tests demonstrated the lack of cytotoxicity towards normal fibroblasts; while NAM grafting generated NPs that stimulated cell proliferation by about 21% in 24 hours of incubation.

*Keywords*: nanoparticles, chitosan, freshwater crayfish, biocompatibility, grafting, acryloyl morfoline, n-vinylacetamide, dimensional optimization

#### INTRODUCTION

An essential element in the development of novel medical devices involved in drug delivery, as well as in detection and isolation of tumours, is represented by nanoparticles (NPs) incorporating biomaterials. This explains the informational explosion of theoretical and applicative studies dedicated to the synthesis of NPs. Recently, special attention has been devoted to the manufacture of NPs from natural polymers, with improved/targeted properties by chemical modification. In this category, polysaccharides stand out, on the one hand due to their biocompatibility, and on the other, due to their ability to structure in (quasi)globular systems with

dimensions that can be regulated by process parameters, such as pH, stirring speed, synthesis temperature vs. action temperature.<sup>1-7</sup>

Chitosan is one of the most promising materials for such applications. Obtained from the chitin of the exoskeletons of crustaceans, shrimps and insects, as well as from yeasts and fungi, chitosan is a natural polysaccharide with a cationic charge,<sup>8</sup> which stands out due to its bioactivity specific defined by biocompatibility, biodegradability, as well as its flexibility in surface modification and the of its obtaining and chemical simplicity modification techniques. Although extremely attractive in composition and functionality, in

relation to the source of extraction, chitosan is characterized by a wide range of molecular mass which is an inconvenience reproducibility of the synthesis and final properties of the material. The multitude of studies demonstrate that high molecular masses accompanied by high values of the degrees of deacetylation (DDA) limit the uses of chitosan because of its low solubility in aqueous environments, hence inherent difficulties in handling and uniformity in active medical formulations. The reduction of the molecular weight stimulates the active capacity particular, the efficiency of incorporating active therapeutic principles), favouring the formation of small sized NPs.9

An important issue in the handling and modification of chitosan substrates is its potential degradation. It is already known that the degradation of chitosan is catalysed by lipases, chitinase, chitinase deacetylase, lysoses, proteases, collagenase, chitosanase and beta-Nacetylhexosaminidase.<sup>10</sup> However, biodegradation process is faster at DDA values less than 70%. In addition, although a natural product, its cytotoxicity is determined by its dimensions. 11,12 molecular Thus, obtaining reliable and viable NPs is still a challenge to harmonize the optimal M<sub>W</sub>-DDA. Another difficulty in manufacturing modified chitosan NPs is related to behavioural peculiarities in relation to the nature of the cross-linking/structuring agent: covalent glutaraldehyde cross-linking has a faster degradation compared to ionic tri-polyphosphate (TPP).<sup>13</sup> Furthermore, facilitating access to the amine group affects the degradation of chitosan: N-stearoyl chitosan degrades much compared to chitosan.14

The biocompatibility of chitosan with living tissues is the result of the changes it undergoes during destructive microbial action: slow fragmentation into amino-sugar sequences, completely absorbed by the living organism. On the other hand, due to its compositional-configurational structure, chitosan has a high antimicrobial capacity and absorbs heavy toxic ions (e.g., mercury, cadmium, lead, etc.). Moreover, its good adhesion, coagulation capacity and immunostimulating activity are remarkable.

Ionotropic gelation/polyelectrolyte complexation continues to excite the scientific world for the preparation of NPs, primarily due to the simplicity of the procedure carried out under mild conditions. Moreover, unlike covalent

cross-linking, it is a reversible process based on electrostatic interactions of participants, thus avoiding the potential toxicity that accompanies chemical cross-linking due to the reagents used or other undesirable effects.<sup>17</sup> In the most general case, ionotropic gelation develops by direct interaction of an ionic polymer with the opposite charge ion to initiate cross-linking. Unlike simple ions, the interaction of polyions with opposite charge ions cannot be completely explained by the principle of electro-neutrality. The network's three-dimensional structure, the presence of other functional groups, as well as the interactions with the synthesis medium influence the conjugation ability with the oppositely charged functions and provide selectivity to the structuring process.

Tripolyphosphate (TPP) is a polyanion, which can interact with cationic CS through electrostatic forces. The cross-linking density varies as a function of the number of charged TPP ions, as well as of the ionization degree of chitosan. Both factors govern the formation of TPP-chitosan ionic bonds. While in acidic pH media (<4), the degree of TPP loading decreases and the chitosan' free amine groups are protonated, slightly decreasing the cross-linking density, in basic media (pH=9) the phenomenon depends on the amine groups' neutralization by deprotonation and on the decrease of chitosan's ionization degree.

The presence of hydrosoluble salts in the reaction mixture (NaCl, CaCl<sub>2</sub>, AlCl<sub>3</sub>) changes the surface charge of the precipitate, decreasing the efficiency of particle wetting by promoting the interactions of TPP ions with cations.<sup>18</sup> With monovalent cations, a relative constancy of the cross-linking degree is noted, without promoting particle aggregation, while when using salts of biand trivalent metal ions, the cross-linking degree decreases, enhancing the electrostatic interactions with the protonate amino groups, thus leading to the formation of larger sized particles. Similar demonstrated behaviour was for acrylamide hydrogels.<sup>19</sup>

The aim of this study has been to optimize the procedure for obtaining NPs from a novel type of chitosan – extracted from freshwater crayfish – as well as its derivatives obtained by grafting with MA, VBC, NAM, NMNVA, MA-VBC and NAM-NMNVA copolymers.

### **EXPERIMENTAL**

#### Materials

The biomaterial substrate subjected to chemical modification was medium molecular weight chitosan

(190÷310 KDa, with the deacetylation degree (DDA) around 75-85%, purchased from Sigma-Aldrich) and freshwater crayfish (CF) chitosan obtained in our laboratory (medium molecular weight 530 KDa; DDA=93%). Cerium sulphate (Ce(SO<sub>4</sub>)<sub>2</sub>), anhydrous, used as grafting initiator, was purchased from Sigma-Aldrich, and used without further purification.

The monomers used for chitosan grafting were as follows: 4-vinyl benzyl chloride (VBC 3;4-isomers mixture (6/4), 97% purity, used without further purification); maleic anhydride briquettes (MA) used after recrystallization; 4-acryloylmorpholine (NAM) and N-methyl N-vinyl-acetamide (NMNVA), with 99% purity, used without purification; all purchased from Sigma-Aldrich.

The solvents for the syntheses were: 1,4-dioxane (D) anhydrous (99.8% purity) and acetic acid, from Sigma-Aldrich, used without further purification; toluene (99% purity) from Chimopar SA, used as received. Sulphuric acid (98%w/w) from Sigma-Aldrich, without further purification, was used for preparing the initiator solution; methanol (MOH) and acetone from Chimreactiv SRL (99.92% purity) was used as supplied. Sodium triphosphate pentabasic (TPP), *purum* p.a., ≥98.0%, from Sigma-Aldrich, was used as cross-linking agent; and 1N aqueous sodium chloride solution was used as electrolytic additive.

#### Nanoparticle synthesis procedure

The synthesis procedure involved a few steps:<sup>20-24</sup>

- i) Chitosan/modified chitosan samples were dissolved in an aqueous solution of acetic acid (0.5M) with the final concentration of 0.1 mg/mL.
- ii) After solubilisation (under stirring for 24 hours at room temperature), the samples were filtered (Millipore 0.45 micron filter);
- iii) Dissolution of TPP in water, filtration and cooling to 2-4 °C.
- iv) The solutions from steps (ii) and (iii) were mixed under stirring, respecting the following molar ratios between chitosan amine groups and the amount of TPP: 1.5/1, 1/1, 1/0.75: 1/0.5. Stirring was continued for 10 min, when a suspension was obtained. The suspension was centrifuged (30 min at 15300 rpm), and the obtained precipitate was washed with deionised water several times. The crude product was purified by lyophilisation (48 h at -80 °C).

The only variables of the procedure were the formulation parameters, to highlight their influence on the particle size and distribution (TPP concentration, chitosan type, degree of deacetilation).

## Characterization methods FTIR-ATR Analysis

The spectra of grafted chitosan were obtained with a Tensor 37 Bruker spectrophotometer (Wordstock, NY, USA), equipped with an ATR Golden Gate unit, in the range of 400-4000 cm<sup>-1</sup>.

#### Dimension analysis and surface charge of NPs

Dynamic light scattering (DLS), also known as photonic correlation spectroscopy or quasielastic light scattering, and zeta potential emerged as simple techniques to investigate the hydrodynamic size and surface charge of NPs, respectively.<sup>25,26</sup> DLS can be used to measure average size and polydispersity index, estimated from the autocorrelation functions.

A Zetasizer NanoSeries (ZEN 3600) from Malvern Instruments was used. Three measurements were performed for each sample, the final result representing their average. All mean particle size and polydispersity index values were expressed as the mean  $\pm$  standard deviation (S.D.).

Zeta potential (ZP) is an important parameter that characterizes NPs (in fact, all colloidal systems). Its value can be positive or negative, and is indicative of the stability of the NPs in the given environment. At low values of zeta potential, the system is unstable and the NPs can cluster and precipitate. As a rule, nanosuspensions with high positive charges have good stability for a potential above +10 or below -10, while suspensions with potential values in the range -10 +10 show a high tendency of aggregation, thus, have low stability. A minimum of three sample dilution measurements were performed for each sample.

## Scanning electron microscopy (SEM) and transmission electron microscopy (TEM)

Chitosan particles separated by centrifugation and lyophilized (Liobras, L101) were morphologically characterized by SEM, using a LEO440i Scanning Electron Microscope (England), equipped with a field emission gun (FEG) electron source, with a resolution of 1.2 nm, and an energy-dispersive X-ray spectrometer (EDS), with a resolution at MnK of 133 eV. For surface analysis, the samples were gold-coated for 80 seconds, to ensure good electrical conductivity.

To visualize the particles, transmission electron microscopy (TEM) was performed using a Philips TEM CM10 (Eindhoven, Netherlands), fitted with a bottom mounted TVIPS TEM Cam F416 camera. For this purpose, 10  $\mu L$  of the sample was diluted in water (1:100 v/v), then 10  $\mu L$  of the diluted sample was mixed with 10  $\mu L$  of 1% (w/v) acetic acid for 30 s. 10  $\mu L$  of sample was placed on a copper grid covered with a Formvar® film (200 mesh) for 30 s. Excess liquid was removed using filter paper and the grids were dried in a desiccator for at least 24 hours.

#### In vitro biocompatibility assay (MTS assay)

Human gingival fibroblasts (HGF, CLS Cell Lines Service GmbH, Eppelheim, Germany) were seeded ( $0.5 \times 10^5$  cells/mL) into 96-well plates in  $\alpha$  MEM medium with 10% fetal bovine serum (FBS, both from Gibco, Thermo Fisher Scientific, Waltham, MA USA) and 1% Penicillin-Streptomycin-Amphotericin B mixture (10 K/10 K/25 µg, Lonza, Basel, Switzerland). The samples' biocompatibility was assessed using the

CellTiter 96® AQueous One Solution Cell Proliferation Assay (Promega, Madison, WI USA), according to the manufacturer's instructions and ISO 10993-5 (extract dilution method).

Samples were extracted over 24 h, at 37 °C, in complete cell culture medium at 5 mg/mL. Cells were incubated with fresh complete medium (control) or different concentrations of samples' extracts (250  $\mu g/mL$ , 500  $\mu g/mL$ , 750  $\mu g/mL$ , 1000  $\mu g/mL$ ) for 24 h. MTS absorbance readings were done at 490 nm on a FLUOstar® Omega Microplate Reader (BMG LabTech, Ortenberg, Germany). Experiments were done in triplicate and treated cell viability was expressed as percentage of control cells' viability (means  $\pm$  standard deviation).

## RESULTS AND DISCUSSION Dimension optimization

Previous studies have shown that CS concentration remains a decisive parameter in the synthesis of nanoparticles by the ionotropic gelation method. Thus, generalizing, the concentration of chitosan determines the formation of individualized nanoparticles or large aggregates. At high dilutions (below 1.5 mg/mL),

the formation of individualized nanoparticles is favoured by disrupting the balance between attractive hydrogen bonds and electrostatic repulsions in the CS chains, which may induce a precipitation of particles due to the deficiency of electrostatic repulsions between particles that typically stabilize colloids. Increasing the TPP amount will be a disadvantage, leading to the formation of aggregates. It is worth noting that, at a CS concentration of 2 mg/mL, aggregation occurs, regardless of the amount of TPP (even a very small amount). Based on the rich literature information, for all the samples in this study, a concentration of 1 mg/mL was chosen, favourable to the high and medium molecular weight values, regardless of the DDA value.27-29 Although apparently the mass concentration of the two components (CSS and TPP) seems to be essential, based on the electrostatic interactions that determine the formation of the particles, the present study proposes an analysis based on the molar ratio of the functional groups specific to the two reaction components (see Table 1).

Table 1
Primary characteristics of chitosan nanoparticles obtained in different media at 1500 rpm

Sample	n <sub>NH2</sub> /TPP	DLS	Before lyophilisation		After lyophilisation	
		medium	D (nm)	PDI	D (nm)	PDI
CSS	1:1.5	H <sub>2</sub> O	267	0.384	_	-
	1:1	$H_2O$	1113	1000	-	-
	1:0.75	$H_2O$	219	0.358	237.66	0.322
	1:0.5	$H_2O$	4423	1000	-	-
CF	1:0.75	$H_2O$	360	0.369	=	-
CSS	1:0.75	- Dioxane	-	=	185.00	0.408
CF	1:0.75		-	=	31.70	0.378
CF	1:0.75	- MeOH	-	=	2802.00	1000
CSS	1:0.75		-	-	1258.00	1000

 $M_{WCSS} = 250 \text{ kDa (DDA} = 80\%); M_{WCF} = 530 \text{ kDa (DDA } 93\%); V_{Chitosan} = 5 \text{ mL}; V_{TPP} = 5 \text{ mL}; speed: 1500 \text{ rpm}$ 

The ratio favourable to narrow polydispersion diameters was determined on the commercial chitosan sample using, water dispersion medium at an acidic pH (around 3). By maintaining the chitosan concentration constant and the overall volume value, the TPP quantity variation was used in accordance with the molar ratios mentioned above. After contact, at low TPP concentrations, the resulting mixture has the appearance of a diluted colloidal solution. Increasing TPP concentration induces the "collapse" of chitosan molecules, a phenomenon that involves organization in a particle-like structure. NP stability is specific to an optimum

dimension obtained for the molar ratio  $NH_2/TPP = 1/0.75$ . At the proposed molar range limit values, unstable molecular aggregates appear.

Resuming the CF experiment under identical conditions led to obtaining particles with sizes in the same order of magnitude as the CSS, but a lower dispersion index value (PDI), indicating an almost monomodal population. Although CF has a molecular weight value almost double that of CS, the contact behaviour with TPP is similar, both in size and homogeneity (see Table 1).

It is important to mention that the size, as well as the stability of the particles, is affected by the nature of the medium (polarity index – IP) used in

their manufacture. Thus, dioxane, with a mean polarity index IP = 4.8, disperses aggregates into small particles, characterized by good stability. Although with an almost double  $M_w$  and a high DDA, CF samples develop particles about 6 times smaller than CSS. Using water (IP = 10.2) and MOH (IP = 5.1) as carrier media for particle formation, aggregation, with the generation of aggregates of tens of microns, is favoured, even after lyophilisation (see Fig. 1). In addition, the sizes of the nanoparticles increased as the molecular weight/DDA of chitosan decreased

(Fig. 1). The PDI decreases as the molecular mass increases, even after lyophilisation.

This behaviour is the consequence of the packing mode of the chain and the electrostatic interactions with the dispersion medium. So, as the length of the chain decreases, the number of amino groups on the chain decreases, some of them being coordinated by water molecules, respectively MOH. A sharp decrease in the absolute value of the zeta potential is expected as the molecular weight decreases.

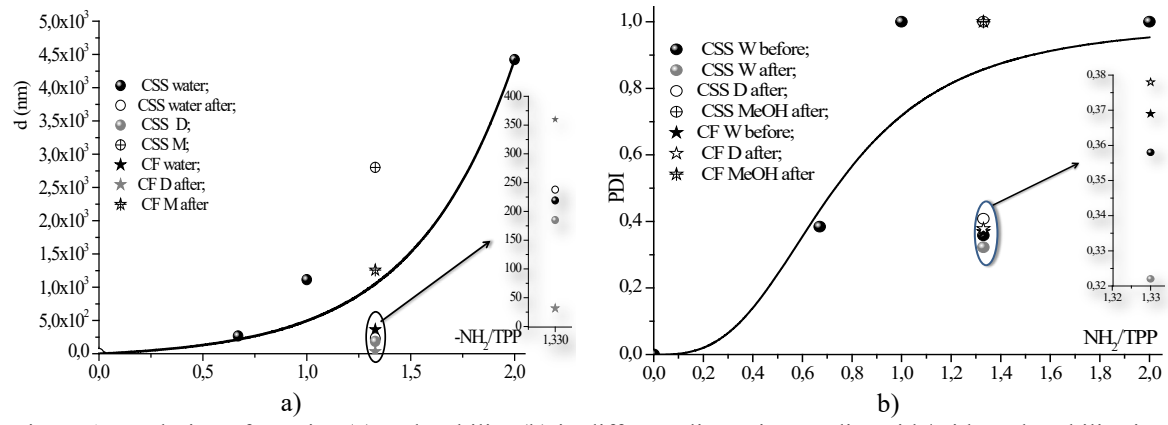


Figure 1: Evolution of NP size (a) and stability (b) in different dispersion media, with/without lyophilisation

#### Characterization by FTIR-ATR analysis

Overall, the PDI values for NPs prepared using CSS were higher compared to those of similar samples of CF.<sup>30,31</sup> The high positive charge density, thanks to its molecular size and DDA value, increases the cross-linking potential with TPP, even in the presence of more powerful electron-acceptor media, favouring the generation of small particles. The structure of macro-chains should not be neglected either: molecular dimensions and high DDA values favour more flexible packaging due to conformational freedom.

If from the conformational point of view, the concentration of the reactants and the processing parameters are essential, the applicative part of the NPs is correlated with the nature of the chemically/biologically active functionalities on their surface. An illustrative analysis is FT-IR spectroscopy. The comparative analysis of CF, TPP and CF-TPP samples, respectively, highlights compositional peculiarities (see Fig. 2). Thus, in the CF spectrum, the broad peaks of medium intensity, in the range of 3750–3300 cm<sup>-1</sup>, are specific to the stretching vibration of the OH group involved in H bonds (3712 cm<sup>-1</sup>) or free

(3478 cm<sup>-1</sup>); and the stretching vibration of N-H free amine (3311 cm<sup>-1</sup>). The broad band with two peaks at about 3000 cm<sup>-1</sup> includes the stretching vibration for the C-H group (found as CH and CH<sub>2</sub> in CF), and at 3067 cm<sup>-1</sup> - the overtone signal of N-H bond of the amide I, II and specific C=O stretching band are situated in the range 1770-1690 cm<sup>-1</sup>, while at 1490 and 1403 cm<sup>-1</sup>, the angular deformation of CH<sub>2</sub> adjacent to C=O group and C-N stretching in amine are recorded. Also, in this region, the N-H stretching vibrations from the primary amine sequence, respectively, the amide II, are overlapping.<sup>32</sup>

The asymmetric stretching of C-O-C from the glycoside bond is found at about 1143 cm<sup>-1</sup>, and the wide band at 1096 cm<sup>-1</sup> is representative for CO stretching vibration.<sup>33</sup> In TPP, the essential bands are found at 1208 cm<sup>-1</sup> (P-O), 1158 cm<sup>-1</sup> (PO<sub>2</sub>), 1099 cm<sup>-1</sup> (PO<sub>3</sub>), and 886 cm<sup>-1</sup> (P-O-P antisymmetric stretching).<sup>34</sup> The integration of TPP into the structure of chitosan involves changes in the fundamental areas of the spectrum. Thus, at 3746 cm<sup>-1</sup>, there is a signal corresponding to the stretching vibration of OH groups involved in hydrogen bonds, while the stretching band of free OH groups widens and has a maximum at

3365 cm<sup>-1</sup>. The peak at 3259 cm<sup>-1</sup> indicates a partial overlap of N-H vibrations over the OH signal. A reduction in the intensity of the amide signals is observed: a net stretch band appears at 1745 cm<sup>-1</sup> (C = O), respectively, 1637 cm<sup>-1</sup>, and amide II is evident at 1534 cm<sup>-1</sup>.

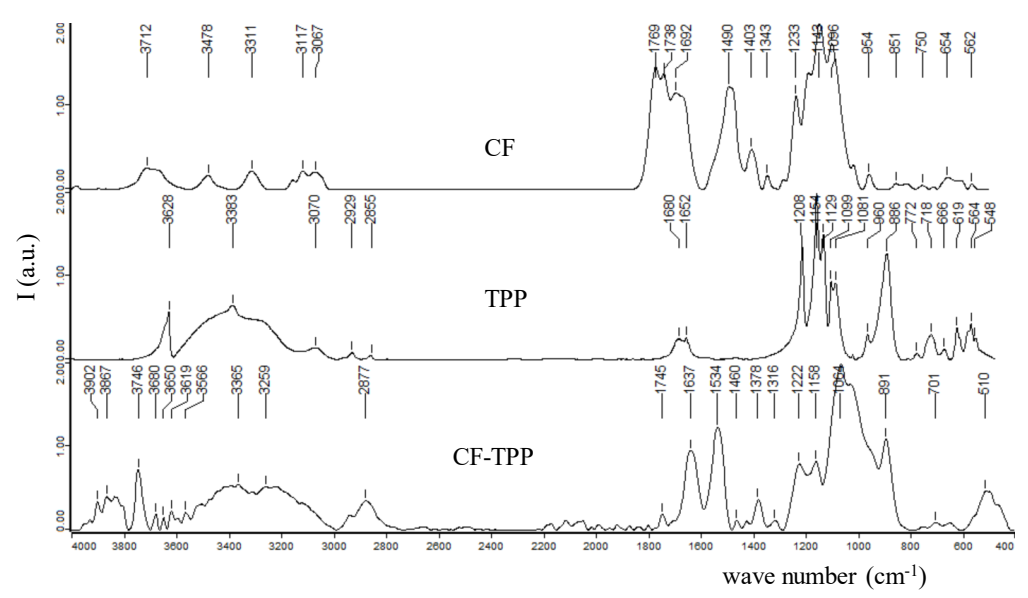


Figure 2: FT-IR spectra of CF nanoparticles

On the other hand, the specific vibration of the TPP is affected: the peak from 1208 cm<sup>-1</sup> shifts to 1222 cm<sup>-1</sup> due to the cross-linking of CF with TPP. All these spectral changes support particle formation based on intra- and intermolecular interactions between CF and TPP.<sup>35-38</sup>

## Structural-dimensional characteristics of chitosan and derivative NPs

The physico-chemical properties of nanomaterials determine their behaviour in the biological environment. 39,40 Surface charge and particle size are the factors most frequently cited as being responsible for a range of biological effects of NPs, including cellular uptake, toxicity and dissolution. 41-43 At the same time, these parameters are defining in the drug release profile, considering the fact that biological matrices modify these two vital characteristics of NPs through different mechanisms (for example, protein adsorption that causes the characteristic corona).44-48

Figure 3 highlights the variation of the NP size in relation to the contact time during the ionic gelation with TPP of the samples: chitosan, chitosan in the presence of NaCl, as well as chitosan grafted with MA, VBC, MA-VBC; NAM, NMNVA and NAM-NMVA, respectively.

During the ionotropic gelation of chitosan, the first 5 hours are characterized by the formation of aggregates with dimensions of approximately 5 μm, which disperse after gelation, with a weak tendency to aggregate in the following 22 hours, stabilizing at around 1.3 µm. The electrolytic addition of NaCl in the reaction medium diminishes the initial aggregation in the first 5 hours, subsequently having the same dimensional stabilization tendency as in the aqueous medium, with a threshold at 2 µm (Fig. 3 (a)). The initial aggregation can be explained by the simultaneous change in the degree of TPP loading and ionization of the NH<sub>2</sub> groups of chitosan, until reaching thermodynamic equilibrium, favouring a practically constant degree of TPP-NH<sub>2</sub> interaction.

The assessment of the dimensional stability of these particles requires the correlation of the surface potential with the PDI (Fig. 3): in the absence of the electrolytic addition, the stabilization is performed after about 7 hours (PDI = 0.89; zeta potential = 25 mV); so the particles remain positively charged, stabilizing at a certain

size, determined by the ionic strength of the

environment.

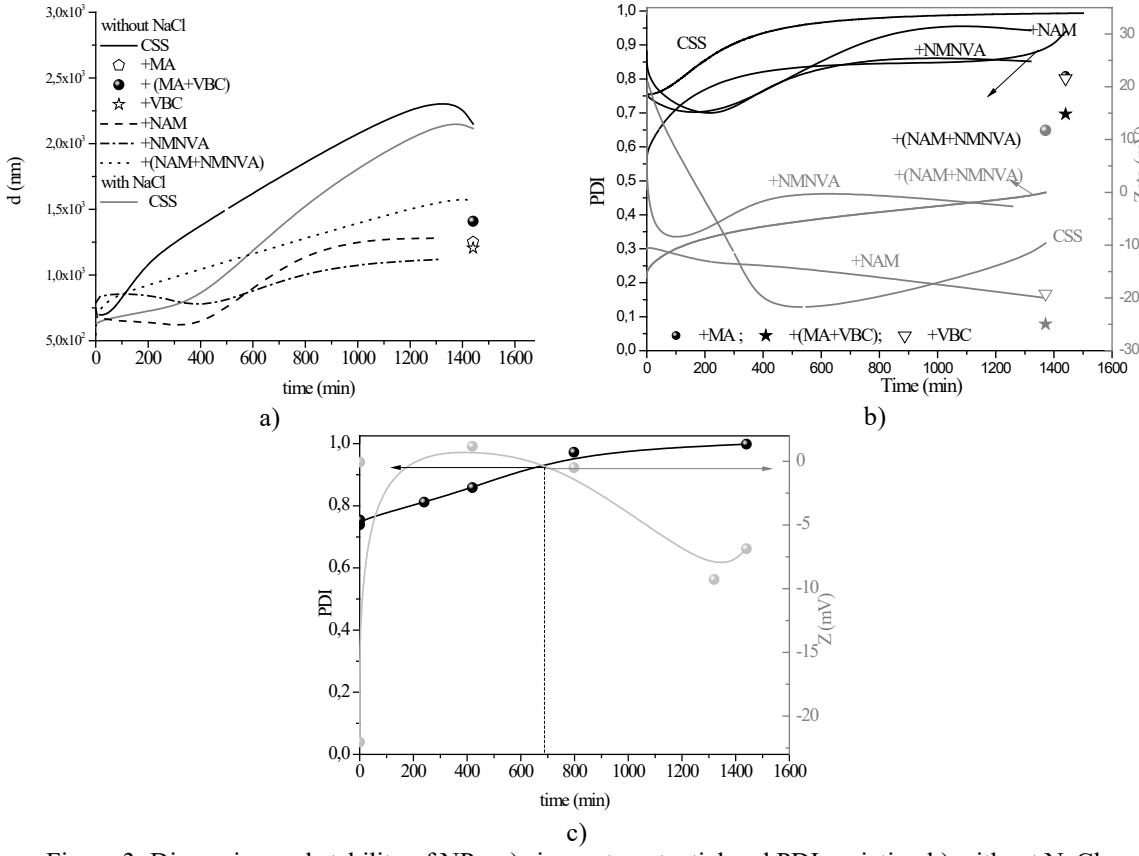


Figure 3: Dimension and stability of NPs: a) size; zeta potential and PDI variation b) without NaCl, and c) with NaCl

In the case of chitosan derivatives (Fig. 3 (a, b)), the chemical nature of the graft sequence particularizes the dimensional values: for NAM, the particle size reaches about 500 nm in the first 6 hours; NMNVA enables a size of about 800 nm in 10 contact hours, which is capped by about 885 nm in 12-15 hours. Chitosan grafting with MA, VBC and its copolymer, complies with the same dimensional order: d<sub>MA-VBC</sub>>d<sub>MA</sub>>d<sub>VBC</sub>. In the case of grafting monomers with segmental rigidity and extended dipole (MA and, respectively, NMNVA), a higher dimensional value is noted, as a consequence of the higher specific molar volume of the units/macromolecular chain attached to chitosan, which determine, through stericelectrostatic repulsions, a slightly lower degree of crosslinking. Thus, when grafting MA-VBC and respectively NAM-NMVA pairs, the increase in particle size is evident, with a higher value in the case of MA-VBC due to the rigidity of the chains of the two monomers – the alternating type – as well as the steric stiffening imposed by the segmental geometry.

When grafting NAM, NMNVA and their copolymer (Fig. 3 (b)), the PDI and the sign of the zeta potential change: NAM: PDI  $\cong$  0.9; zeta = -17; NMNVA PDI = 0.81, zeta = -0.86; copolymer: PDI  $\cong$  0.83; zeta  $\rightarrow$  0 mV.

Relatively high PDI values can be explained by the presence of multiple dimensional pathways the substrate and/or macrocatene fragmentation, as a result of the interaction with TPP in the reaction medium. On the other hand, surface charge is the consequence of the nature of the grafted sequence: NAM is an amide structure, similar to the glycoside bond of chitosan, while NMNVA is an acyclic amide sequence with extended dipole, and at the level of the copolymer (zeta 0 mV), there is an energetic compensation that may be the consequence of some chains with equimolar composition NAM/NMNVA. The modification by grafting with NAM, NMNVA and their copolymer diminishes the PDI value and modifies the sign of the zeta potential, promoting a positively charged surface.

#### Surface morphology of NPs

The characterization of the material through the two recognized imaging techniques – SEM

and TEM – was carried out in order to provide an insight into the morphology and size profile of NPs synthesized from CF (Fig. 4).

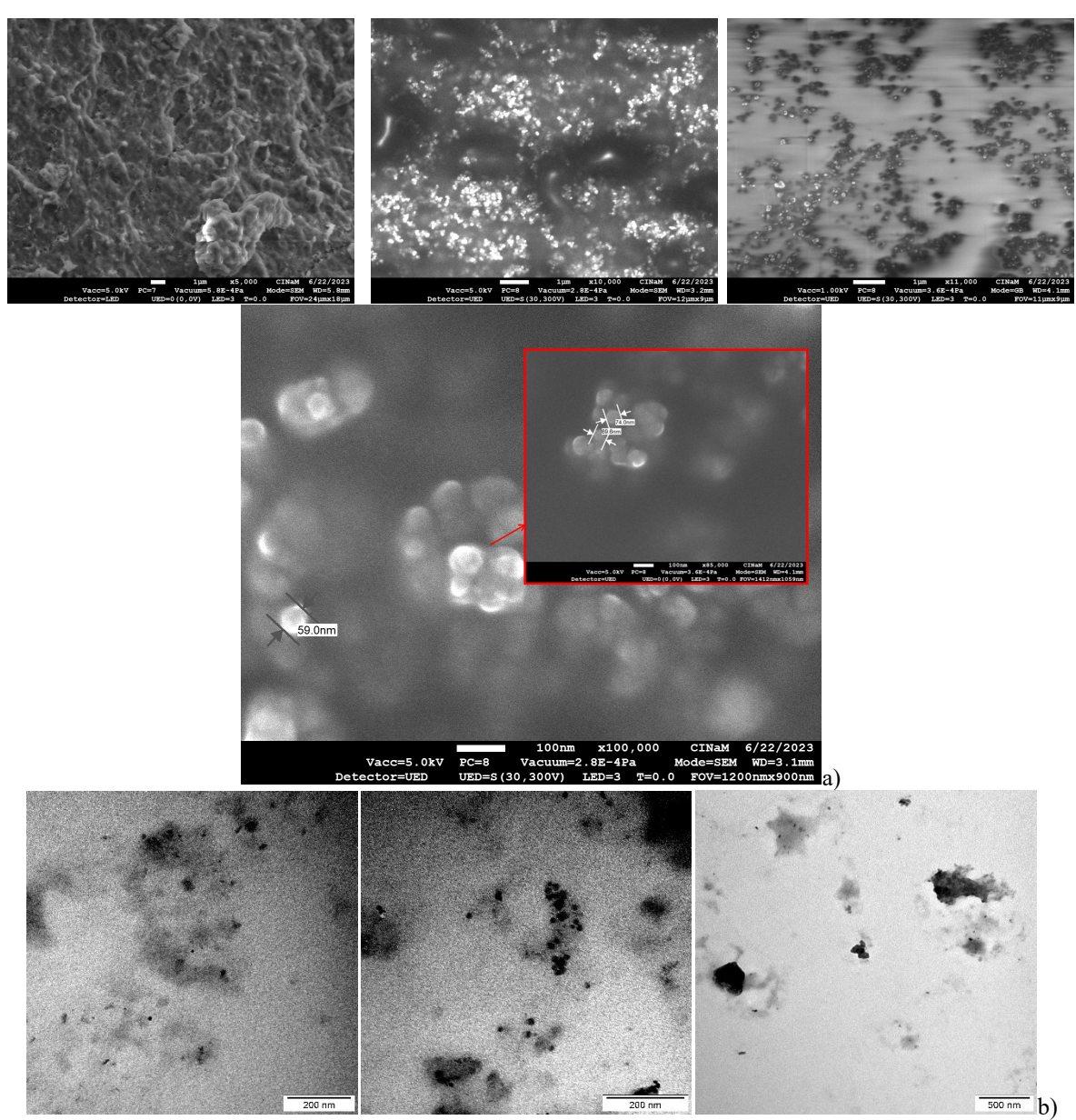


Figure 4: (a) SEM and (b) TEM micrographs of NPs

According to the SEM images (see Fig. 4 (a)), the material assembly reveals homogeneous surfaces, without aggregation, resulting from the formation of spherically shaped nanoparticles. The lack of aggregates is undoubtedly an indication of the coating properties of CF. In addition, the smooth spherical shape, consistent with the data reported in the literature, demonstrates what was previously discussed in the DLS analysis of NPs:<sup>49,50</sup> a strong interaction between the reactive groups of the formulation components, which contributes to the formation

of NPs. The size of the NPs is found in the range of 59-74 nm, which underlines the potential use in tumour therapies, where one of the major factors for isolation and treatment is the size below 200 nm. <sup>51</sup> Complementarily, TEM analysis reconfirms the DLS and SEM results.

#### In vitro biocompatibility of NPs

In vitro biocompatibility testing (MTS assay) required the use of a 5 mg/mL sample extract, subsequently diluted fivefold. The testing of each sample was carried out in complete culture

medium (Alpha-MEM medium + 10% fetal bovine serum + 1% antibiotic-antimycotic), at a dilution of the extract in the range of 25-100% and the incubation of 5,000 HGF cells/well (human gingival fibroblasts) for 24 h. The experiments were done in triplicate and the viability of the treated cells was expressed as a percentage of the viability of the control cells. Graphical data were expressed as means ± standard deviation.

The in vitro assay showed that the samples' extracts were not cytotoxic for normal fibroblasts at the tested concentrations (Fig. 5). Furthermore, CF-NAM extracts stimulated the proliferation of normal fibroblasts by 21% during 24 h incubation. This behaviour can be justified, on the one hand, by the conformation of the novel type of chitosan and, on the other, probably by the hydrophilicity increase, which stimulated the interaction of the morpholine groups with the glycosidic sequences.<sup>52</sup>

Thus, the lack of cytotoxicity for CF NPs and derivative CF NPs demonstrates that such NPs are safe alternatives for drug delivery.

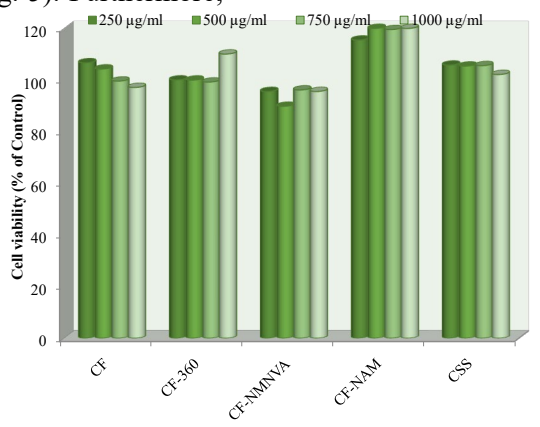


Figure 5: Biocompatibility of NPs: CF powder; CF-NPs (CF-360); CF grafted with NMNVA (CF-NMNVA); CF grafted with NAM (CF-NAM) and commercial chitosan (CSS) on normal fibroblasts over 24 h

#### **CONCLUSION**

In this study, nanoparticles from a new type of chitosan, with high molecular weight and DDA values, were successfully synthesized and dimensionally optimized. The characterization of NPs was achieved using specific materials science techniques (FT-IR, DLS, SEM, TEM), which demonstrated the compositional morphological structure, based on which, the potential use of synthesized nanoparticles in drug delivery, the isolation and therapy of tissue tumours is profiled. Moreover, biocompatibility tests demonstrate, in addition to the lack of cytotoxicity for all the analyzed formulations, the stimulation of fibroblast proliferation by the use of CF-NAM derivative.

Further studies for in vivo evaluation of the most promising formulations are underway and forthcoming results will be reported.

#### REFERENCES

T. K. Giri, A. Alexander, T. K. Barman and S. Maity, Curr. Drug Deliv., 13, https://doi.org/10.2174/1567201812666150603151250

- <sup>2</sup> T. K. Giri, P. Mukherjee, T. K. Barman and S. Maity, Int. J. Biol. Macromol., 88, 236 (2016), https://doi.org/10.1016/j.ijbiomac.2016.03.056
- T. K. Giri, T. K. Barman and S. Maity, Anticancer Med.Chem., 16, 816 https://doi.org/10.2174/1871520616666151116121821
- T. K. Giri, K. Pramanik and S. Maity, Anticancer 1669 Agents Med. Chem., 7. (2017).https://doi.org/10.2174/1871520617666170419121322
- A. Rubinstein, Drug Dev. Res., 50, 435 (2000), https://doi.org/10.1002/1098-2299(200007/08)50:3/43.0.CO;2-5
- T. F. Vandamme, A. Lenourry, C. Charrueau and J. Chaumeil, Carbohyd. Polym., 48, 219 (2002), https://doi.org/10.1016/S0144-8617(01)00263-6
- V. R. Sinha and R. Kumria, Int. J. Pharm., 224, 19 (2001), https://doi.org/10.1016/S0378-5173(01)00720-
- S. Hajji, I. Tounes, O. Ghorbel-Bellaaj, R. Hajji, R. Rinaudo et al., Int. J. Biol. Macromol., 65, 298 (2014), https://doi.org/10.1016/j.ijbiomac.2014.01.045
- H. Yang and M. Hon, Microchem. J., 92, 87 (2009), https://doi.org/10.1016/j.microc.2009.02.001
- <sup>10</sup> J. Sarvaiya and Y. K. Agrawal, Int. J. Biol. Macromol.. 454 (2015),https://doi.org/10.1016/j.ijbiomac.2014.08.052

11 M. Huang, E. Khor and L. Lim, Pharm. Res., 21, (2004).https://doi.org/10.1023/b:pham.0000016249.52831.a5 <sup>12</sup> P. Taskin, H. Canisag and M. Sen, *Radiat. Phys.* 94, 236 https://doi.org/10.1016/j.radphyschem.2013.04.007 <sup>13</sup> T. Kean and M. Thanou, Adv. Drug Deliv. Rev., **62**, 3 (2010), https://doi.org/ 10.1016/j.addr.2009.09.004 <sup>14</sup> J. Sarvaiya and Y. K. Agrawal, Int. J. Biol. Macromol., **72**, 454 (2015),https://doi.org/10.1016/j.ijbiomac.2014.08.052 <sup>15</sup> A. Polk, B. Amsden, K. De Yao, T. Peng and M. F. A. Goosen, J. Pharm. Sci., 83, 178 (1994), https://doi.org/10.1002/jps.2600830213 <sup>16</sup> L. S. Liu, S. Q. Liu, S. Y. Ng, M. Froix, T. Ohno et al., J. Control. Rel.,43, 65 (1997),https://doi.org/10.1016/S0168-3659(96)01471-X <sup>17</sup> Y. Kawashima, *Chem. Pharm. Bull.*, **33**, 2469 (1985), https://doi.org/10.1248/cpb.33.2469 <sup>18</sup> M. K. Rasmussen, J. N. Pedersen and R. Marie, Commun., 11. 2337 Nat (2020),https://doi.org/10.1038/s41467-020-15889-3 <sup>19</sup> H. R. Norouzi, H. Azizpour, S. Sharafoddinzadeh and A. J. Barati, Chem. Petrol. Eng., 45, 13 (2011), https://doi.org/10.22059/JCHPE.2011.23478 N. Sawtarie, Y. Cai and Y. Lapitsky, Colloids Surf. Biointerfaces, 157, (2017),https://doi.org/10.22059/JCHPE.2011.23478 <sup>21</sup> Y. Huang and Y. Lapitsky, J. Colloid Interface 486. (2017),https://doi.org/10.1016/j.colsurfb.2017.05.055 <sup>22</sup> H. Jonassen, A. L. Kjøniksen and M. Hiorth, Colloid. 919 Polym. Sci., 290, (2012),https://doi.org/10.1007/s00396-012-2604-3 <sup>23</sup> S. Kunjachan and S. Jose, Asian J. Pharm., 4, 148 (2010), https://doi.org/10.22377/ajp.v4i2.220 N. Van Bavel, T. Issler, L. Pang, M. Anikovskiy and E. J. Prenner, Molecules, 28, 4328 (2023), https://doi.org/10.3390/molecules28114328 <sup>25</sup> M. A. Digman and E. Gratton, Annu. Rev. Phys. Chem., **62**, 645 (2011),https://doi.org/10.1146/annurev-physchem-032210-103424 <sup>26</sup> R. Dzakpasu and D. Axelrod, *Biophys. J.*, **87**, 1279 (2004), https://doi.org/10.1529/biophysj.103.033837 M. J. Alonso, P. Calvo, C. Remunan-Lopez and J. L. Vila-Jato, J. Appl. Polym. Sci., 63, 125 (1997), https://doi.org/10.1002/(SICI)1097-4628(19970103)63:1<125::AID-APP13>3.0.CO;2-4 <sup>28</sup> W. Fan, W. Yan, Z. Xu and H. Ni, Colloids Surf. B Biointerfaces, 90. 21 (2012),http://dx.doi.org/10.1016/j.colsurfb.2011.09.042 <sup>29</sup> Q. Gan, T. Wang, C. Cochrane and P. McCarron, Colloids Surf. B Biointerfaces, 44, 65 (2005), http://dx.doi.org/10.1016/j.colsurfb.2005.06.001 <sup>30</sup> N. K. Al-Nemrawi, S. S. M. Alsharif and R. H. Dave, Int. J. Appl. Pharm., 10, 6060 (2018), https://doi.org/10.22159/ijap.2018v10i5.26375

<sup>31</sup> S. A. Algharib, A. Dawood, K. Zhou, D. Chen, C. Li et al., J. Mol. Struct., 1252 https://doi.org/10.1016/j.molstruc.2021.132129 <sup>32</sup> A. Pawlak and M. Mucha, *Thermochim. Acta*, **396**, (2003),https://doi.org/10.1016/S0040-153 6031(02)00523-3 E. Pretsch, P. Bühlmann and M. Badertscher (Eds.), "Structure Determination of Organic Compounds", 5th ed., Springer-Verlag GmbH, 2020, pp. 327-358, https://doi.org/10.1007/978-3-662-62439-5 <sup>34</sup> C. Pan, J. Qian, C. Zhao, H. Yang, X. Zhao et al., 241, Carbohvd. Polym., 116349 (2020),https://doi.org/10.1016/j.carbpol.2020.116349 35 M. R. De Moura, F. A. Aouada, R. J. Avena-Bustillos, T. H. McHugh, J. M. Krochta et al., J. Food 448 Eng., 92, https://doi.org/10.1016/j.jfoodeng.2008.12.015 <sup>36</sup> N. Mohammadpour Dounighi, R. Eskandari, M. Avadi, H. Zolfagharian, A. MirMohammad et al., JVATiTD. 18. 44 https://doi.org/10.1590/S1678-91992012000100006 A. L. de Pinho Neves, C. C. Milioli, L. Müller, H. G. Riella, N. C. Kuhnen et al., Colloids Surf., A: Physicochem. Eng. Aspects, 445, 34 https://doi.org/10.1016/j.colsurfa.2013.12.058 <sup>38</sup> J. Antoniou, F. Liu, H. Majeed, J. Qi, W. Yokoyama et al., Colloids Surf., A: Physicochem. Eng. 465. 137 https://doi.org/10.1016/j.colsurfa.2014.10.040 <sup>39</sup> L. Treuel, K. A. Eslahian, D. Docter, T. Lang, R. Zellner et al., Phys. Chem. Chem. Phys., 16, 15053 (2014), htpps/doi.org/10.1039/C4CP00058G <sup>40</sup> A. Akbarzadeh, M. Samiei and S. Davaran, Nanoscale Res. Lett., 7, 144 (2012),https://doi.org/10.1186/1556-276X-7-144 <sup>41</sup> E. Fröhlich, *Int. J. Nanomed.*, 7, 5577 (2012), https://doi.org/10.2147/IJN.S36111 <sup>42</sup> S. Bhattacharjee, I. M. C. M. Rietjens, M. P. Singh, T. M. Atkins, T. K. Purkait et al., Nanoscale, 5, 4870 (2013), http://dx.doi.org/10.1039/C3NR34266B <sup>43</sup> J. L. Axson, D. I. Stark, A. L. Bondy, S. S. Capracotta, A. D. Maynard et al., J. Phys. Chem. C, 119. 20632 (2015),https://doi.org/10.1021/acs.jpcc.5b03634 <sup>44</sup> E. Blanco, H. Shen and M. Ferrari, Nat. Biotechnol., 33, 941 (2015),https://doi.org/10.1038/nbt.3330 <sup>45</sup> R. Singh and J. W. Lillard, Exp. Mol. Pathol., 86, 215 (2009), http://doi/ 10.1016/j.yexmp.2008.12.004 <sup>46</sup> H. Takedatsu, K. Mitsuyama and T. Torimura, World J. Gastroenterol., 21, 11343 http//doi/10.3748/wjg.v21.i40.11343 <sup>47</sup> S. Ritz, S. Schöttler, N. Kotman, G. Baier, A. Musyanovych et al., Biomacromolecules, 16, 1311 (2015), https://doi.org/10.1021/acs.biomac.5b00108 <sup>48</sup> M. Lundqvist, *Nature Nanotech.*, **8**, 701 (2013), https://doi.org/10.1038/nnano.2013.196

<sup>49</sup> R. Ghasemi, M. Abdollahi, E. E. Zadeh and K. Khodabakhshi, *Sci. Rep.*, **8**, 9854 (2018), https://doi.org/10.1038/s41598-018-28092-8
<sup>50</sup> A. Lucero and C. Alejandra, *RSC Adv.*, **9**, 8728 (2019), http://dx.doi.org/10.1039/C9RA00821G
<sup>51</sup> A. V. A. Mariadoss, R. Vinayagam, V. Senthilkumar, M. Paulpandi, K. Murugan *et al.*, *Int. J. Biol. Macromol.*, **130**, 997 (2019), https://doi.org/10.1016/j.ijbiomac.2019.03.031
<sup>52</sup> ISO 10993-5:2009, Biological evaluation of medical devices – Part 5: Tests for *in vitro* cytotoxicity, International Organization for Standardization, Geneva, Switzerland, 2009